Self-seeded quantum-dash laser based 5 m–128 Gb/s indoor free-space optical communication

M. A. Shemis[1], A. M. Ragheb[2], E. Alkhazraji[3], M. A. Esmail[2], H. Fathallah[4], S. Alshebeili[2,5], and M. Z. M. Khan[1,*]

[1]*Optoelectronics Research Laboratory, Electrical Engineering Department, King Fahd University of Petroleum and Minerals, Dhahran 31261, Saudi Arabia*

[2]*KACST-TIC in Radio Frequency and Photonics for the e-Society (RFTONICS), Riyadh 11421, Saudi Arabia*

[3]*Department of Electrical and Electronics Engineering Technology, Jubail Industrial College, Jubail 31951, Saudi Arabia*

[4]*Computer Department of the College of Science of Bizerte, University of Carthage, Tunis 1054, Tunisia*

[5]*Electrical Engineering Department, King Saud University, Riyadh 11421, Saudi Arabia*

**Corresponding author: zahedmk@kfupm.edu.sa*

Received June 13, 2017; accepted August 11, 2017; posted online September 4, 2017

We demonstrate an indoor 5 m free-space optical wireless coherent communication in mid L-band (1606.7 nm) by employing a tunable self-seeded InAs/InGaAlAs/InP quantum-dash (Qdash) laser as a subcarrier generator for 128 Gb/s dual-polarization quadrature phase shift keying (DP-QPSK) modulation signal. The bare Qdash laser diode displays ∼6 nm self-locked Fabry–Perot mode tunability with ∼30 dB side mode suppression ratio (SMSR) and ∼10 dBm mode power across the tuning range, thus encompassing ∼10 modes with an achievable capacity of 1.28 Tb/s (10×128 Gb/s) and potentially qualifying the source requirements for future access networks.

OCIS codes: 060.2605, 250.5590, 140.5960, 140.3520.
doi: 10.3788/COL201715.100604.

Free-space optical (FSO) wireless communication has recently reaped major attention as a complement, backup, and/or substitute for fiber networks due to several advantages, such as high degree of flexibility, reliability, scalability, security, and, importantly, low initial capital cost, while providing high-speed connectivity, comparable to the fiber infrastructure. Data rates as high as 320 Gb/s using dual-polarization (DP) 16 array quadrature amplitude modulation (QAM)[1] over 100 m, and 100 Gb/s, using single-polarization quadrature phase shift keying (SP-QPSK)[2] over 120 m outdoor-FSO links, have been recently reported using 1550 nm external cavity lasers (ECLs) and distributed feedback (DFB) lasers. Moreover, a fiber-free-space hybrid system is being considered as a potential platform to mitigate the environmental difficulties of fiber deployment in a wired network, for instance, across bridges, rivers, highways, etc. In this regard, a hybrid system with a 22 km single mode fiber (SMF)/100 m outdoor FSO[3] and a 40 km SMF/80 m outdoor FSO[4] are reported. The corresponding data capacities of 12×72 and 16×100 Gb/s, using SP-16-QAM and DP-QPSK formats, respectively, are reported in the C-band region, corroborating the potential of FSO for future access networks.

Recently, indoor-FSO communication is also gaining popularity as a substitute for the long and high density fiber connections, inside data centers (DCs)[5], and high performance computing (HPC)[6] for better rerouting flexibility and relieving the load on wireless fidelity (Wi-Fi) and radio frequency (RF) networks with a lower chance of channel interference. In fact, card-to-card optical wireless interconnects have also been reported with this transport system. Furthermore, the hybrid transmission system with a 20 km SMF and 17.5 m indoor FSO was also demonstrated at 1310, 1490, and 1556 nm by transmitting 0.63 Gb/s data signals together with the community access television (CATV) system signal. These demonstrations affirm the new perspectives of the fiber-FSO hybrid system in addressing the next generation of broadband access requirements.

Recently, the realization of passive optical networks (PONs) by this hybrid technology with potential deployment in the more flexible and scalable fiber-to-the-home (FTTH) network and leveraging on the shared optical platform[3,4] is already garnering attention as a plausible next-generation access infrastructure. On other front, indoor-FSO-based wavelength division multiplexed (WDM) PON-based interconnects is an appealing solution for optimum inter- and intra-rack communication in DC and HPC systems. In this respect, colorless WDM-PON, which is based on wavelength independent sources by exploiting the injection-locking technique, is a desirable choice to realize the FSO infrastructure[7]. Besides, integration of injection-locked unified transceivers in this network would significantly reduce the capital expenditure (CAPEX) of the system, as has been actively researched in the fiber-based network[8]. This opens a new paradigm for convergence of indoor/outdoor-FSO and injection-locking technologies to address a multitude of future needs of communication and information systems. In particular, the penetration of injection-locked WDM-PON via indoor-FSO technology would enable the

realization of wireless DC and HPC networks with flexibility and scalability.

Different light sources, which directly affect the performance of an optical communication system, have been proposed and demonstrated in WDM-PONs[9]. In particular, very recently, the deployment of a C-band quantum dash (Qdash) active-region-based semiconductor laser source, as a frequency comb in a WDM system[10] or as an external seeding light source in injection-locked WDM-PONs[11], have been investigated with 60×200 and 16×2.5 Gb/s transmission capacities, respectively, thanks to the inherent broadband lasing spectrum offered by this new class of laser diodes (LD) compared to single wavelength DFB lasers[12]. Moreover, we also demonstrated the viability of an externally injection-locked Qdash LD as a tunable transmission source with an ~20 nm locked Fabry–Perot (FP) mode tunability in the far L-band region by exploiting the wide emission range of these nanostructures. We also reported a 100 Gb/s DP-QPSK transmission from this source over a 4 m indoor-FSO link[13] with the potential capacity of 50×100 Gb/s if all of the locked modes are utilized simultaneously.

In this work, we investigated the self-injection-locking scheme on an L-band Qdash LD, which is more attractive with the elimination of an external seeding source. By employing a passive band pass filter (BPF) to selectively feedback a particular FP mode, the self-locking mode tunability of ~6 nm is achieved. Moreover, a mode peak power of ~10 dBm with an ~30 dB side mode suppression ratio (SMSR) in the wavelength range of ~1600–1607 nm is exhibited by the LD. Then, by deploying a single locked mode of 1606.7 nm as a subcarrier, an error-free transmission of 128 and 176 Gb/s of a DP-QPSK signal over a 5 m indoor-FSO link is demonstrated. This work further corroborates the prospects of a tunable self-seeded Qdash LD, which exhibits the additional feature of a unified transmitter and, possibly, a unified transceiver via a Qdash photodiode in future Tb/s indoor-FSO based WDM access networks, thus significantly reducing the CAPEX of the novel network infrastructure.

Figure 1(a) shows the experimental setup of the self-seeding scheme and the FSO communication system that utilizes the InAs/InP Qdash LD. The InAs Qdashes were embedded in an asymmetric InGaAlAs quantum well with four-multilayer active region structure. The bare Qdash LD has a 3 μm ridge width and a 600 μm cavity length and is grown using the molecular beam epitaxy (MBE) technique. More details can be found in Ref. [14]. This Qdash LD was utilized as an optical source in our work after butt-coupling into a lensed SMF with an ~5% (~13 dB) coupling efficiency and biasing at above the threshold current value of $1.1I_{\text{th}}$ ($I_{\text{th}} = 100$ mA), and maintained at a heatsink temperature of 14°C. The device exhibited a single facet fiber coupled power of ~0.5 mW (~−3 dBm). Then, a tunable BPF with ~7 dB insertion loss was utilized in order to filter out a single FP mode. The latter was then fed back via an optical circulator

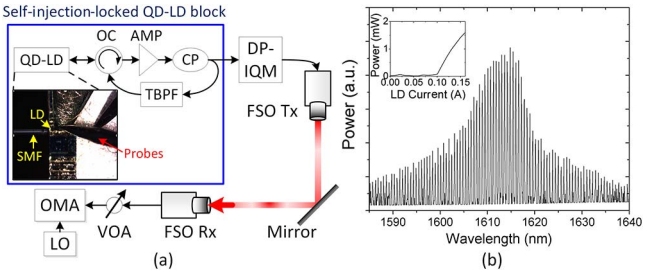

Fig. 1. (a) Utilization of self-injection-locked Qdash LD in FSO communication. (b) Free-running lasing spectrum of Qdash LD at just above the threshold (110 mA). The inset of (b) shows the CW SMF coupled *L-I* characteristics of the laser at a 14°C heatsink temperature. AMP, optical amplifier.

(OC) right into the laser cavity to injection lock the generated photons to match that particular FP mode's phase and wavelength. An erbium-doped fiber amplifier (EDFA) with an ~20 dB gain was utilized to compensate for the coupling loss (~13 dB) and for the BPF insertion loss (~7 dB). Thereafter, a 3 dB optical coupler (CP) was employed in order to equally split the emission, where one half was utilized in the feedback loop. However, in future applications, this self-locking arrangement can be substituted with a customized and tunable single fiber Bragg grating (FBG) for a more convenient and cost-effective installation. The other half of the optical power from the 3 dB CP port, on the other hand, was utilized as a self-injection-locked subcarrier for carrying a pseudo-random binary sequence (PRBS) of the length 2^{11}–1, modulated in DP-QPSK format, using an external DP in-phase quadrature modulator (DP-IQM) with an insertion loss of ~13 dB. The optical signal was then transmitted through a 5 m long FSO channel that was implanted indoor, using two SMF collimators and a mirror with a total channel loss of ~4 dB. This loss was evaluated by transmitting a known power mid L-band light and recording the received power after the collimator. Finally, the received signal was coherently demodulated using an optical modulation analyzer (OMA-N4391A) facilitated with a copy of the subcarrier as a local oscillator (LO) after being attenuated with a variable optical attenuator (VOA) to investigate the receiver sensitivity for a successful transmission.

The free-running lasing spectrum of the Qdash LD, obtained at a 110 mA biasing current, using an optical spectrum analyzer (OSA), displayed a broadband lasing emission coverage of ~1600–1630 nm with a −3 dB bandwidth of ~8–10 nm, as shown in Fig. 1(b). The LD's continuous wave (CW) *L-I* characteristics, obtained at the coupled SMF end, are plotted in the inset of Fig. 1(b). A maximum power of ~2.0 mW was measured from the device before roll off. For the self-injection-locking characterization, two devices of different ridge widths 3 μm × 600 μm and 4 μm × 600 μm were utilized with similar spectral characteristics. Six different FP modes in the range of ~1600–1607 nm were locked for each device. The selectivity of the locked mode was achieved by tuning

the passband and the central wavelength of the BPF along the specified range. This wavelength range is manifested as the intersection between the bandwidth and central wavelength of the BPF and the emission wavelength coverage of the Qdash LD. In other words, the actual number of available modes that can be potentially self-locked is currently limited by the mismatch between the near L-band EDFA and the mid L-band Qdash LD. Figure 2 shows the self-injection-locked FP modes of the 4 μm × 600 μm device, each acting as potential coherent subcarrier of the tunable self-seeded Qdash LD. As the inset of Fig. 2 depicts, the average mode peak power was ∼8.5 dB with an SMSR of ∼30 dB across the tuning range of ∼6 nm. On the other hand, the 3 μm ridge-width device was found to exhibit superior self-locked FP mode peak power value of ∼10 dB, thanks to the better slope efficiency (external quantum efficiency) of the device, while the SMSR and tuning range were found to be similar. In terms of wavelength, the linewidth of each mode was ∼0.05 nm with a mode spacing of ∼0.6 nm, thus corresponding to ∼10 locked modes within the tuning range. The injection ratio (self-injected peak power to the free-running lasing power ratio) was estimated to be ∼−20 dB. From the short term stability test of 20 min on both devices, across all used self-injection-locked subcarriers, the mode power and wavelength were found to be stable with ±0.1 dB and ±0.02 nm variation, respectively. Since the 3 μm device exhibited better mode power characteristics, this device was selected for the subsequent transmission experiments.

Thereafter, one self-seeded FP mode at 1606.7 nm was selected as a subcarrier in the established FSO communication system, shown in Fig. 1(a). As such, the subcarrier was modulated with a 32 Gbaud (128 Gb/s) signal in the DP-QPSK format using a DP-IQM, which was then transmitted through the 5 m long indoor-FSO channel. Therein, the bit-error-rate (BER), estimated from the error vector magnitude (EVM), was measured after demodulating the signal by the OMA. First, the self-seeded subcarrier mode peak power was varied by varying the gain of the EDFA, which in turn altered the injection ratio. The results, plotted in Fig. 3, reveal a minimum injection ratio of ∼−21.5 dB, corresponding to the self-injected mode power of ∼8.5 dBm and SMSR of ∼25 dB, which is required for attaining error-free transmission below the forward error correction (FEC) threshold of 3.8×10^{-3}. Moreover, the SMSR of ≥32 and mode power of >10 dBm of the mode ascertained the BER values of $<1 \times 10^{-5}$, translating to an injection ratio of >∼−20 dB.

Next, the performance of the indoor FSO was further investigated by measuring the BER at different received power values by fixing the mode power to ∼10 dBm (∼−20 dB injection ratio). The values are plotted in Fig. 4, which reveal a minimum receiver sensitivity of −16 dBm that is required to maintain a BER below the FEC threshold. Moreover, Fig. 4 also demonstrates that a successful DP-QPSK transmission of 44 Gbaud (176 Gb/s) is also achieved at a received power of −11 dBm with a 2.1×10^{-3} BER value. The eye and constellation diagrams for the case of 44 Gbaud transmission, in addition to the 32 Gbaud transmission, for both the minimum and maximum received power values are also shown as insets in Fig. 4. Clear constellations and open eye diagrams further demonstrated successful transmission of the DP-QPSK signals, thus paving the road for the deployment of a self-seeded FP Qdash LD as a tunable coherent source in next-generation FSO-WDM-PONs, in which several subscribers are incorporated at a minimum cost by unifying transceivers.

Finally, we estimated the laser spatial power density emitted in free space by taking an ∼0.36 cm diameter of the SMF collimator to be the spot size of the laser assuming a Gaussian beam as a worst-case scenario. With a maximum transmitted peak power of ∼−3 dBm, the

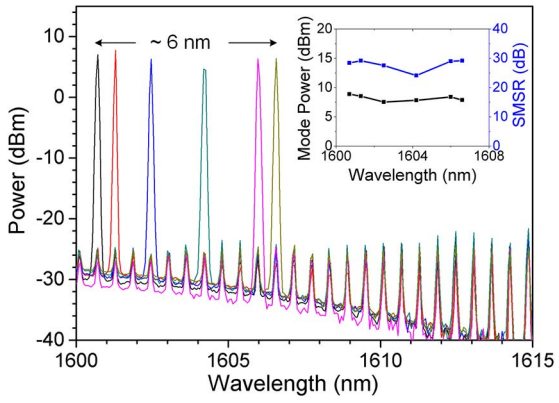

Fig. 2. (Color online) Self-injection locking of different FP modes in the wavelength range of ∼1600–1607 nm, measured at the 2% output of the 2:98 CP. The inset shows the corresponding variation in the mode power and the SMSR across the locked FP modes.

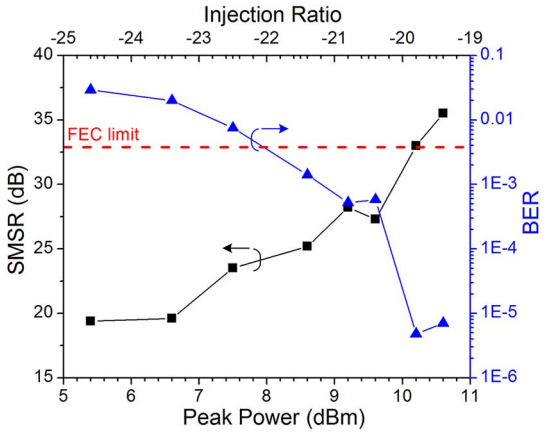

Fig. 3. (Color online) Measured SMSR and BER at different peak powers for the 1606.7 nm self-locked FP mode, and also the corresponding different injection ratio for the 5 m 32 Gbaud (128 Gb/s) DP-QPSK FSO transmission.

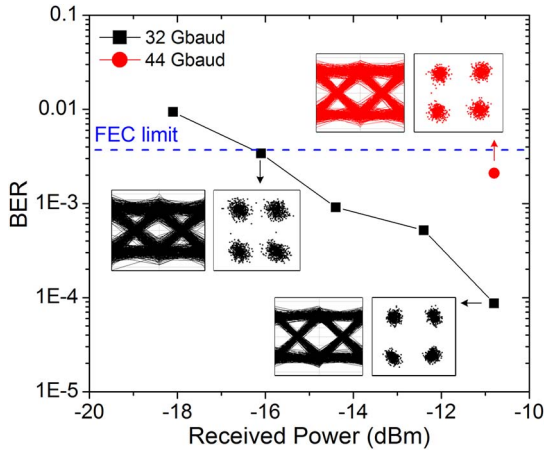

Fig. 4. BER versus received power for 5 m/32 Gbaud and 5 m/44 Gbaud DP-QPSK transmission, utilizing a 1606.7 nm self-seeded FP mode as a sub-carrier. The insets show the corresponding constellation and eye diagrams.

worst-case spatial power density was estimated to be ~4.9 mW/cm^2, which was found to be much less than the 0.1 W/cm^2 IEC 60825-1 standard limit for Class 1 laser classification for distances less than 100 m, thus qualifying the laser operation to be eye safe under all conditions of normal use[15].

In conclusion, we demonstrate the viability of convergent indoor-FSO and injection-locking technologies for future access networks by successful error-free transmission of an externally modulated 128 Gb/s DP-QPSK signal over a 5 m indoor-FSO channel via a single self-locked 1606.7 nm FP mode of a Qdash LD as a subcarrier. We further show the device self-locked mode tunability of ~6 nm, encompassing ~10 modes in the wavelength range of 1600–1607 nm and exhibiting an ~30 dB SMSR and ~10 dBm average mode power. This is the first demonstration, to the best of our knowledge, of a 5 m 128 Gb/s indoor-FSO link at ~1607 nm employing a self-injection-locked Qdash LD.

This work was supported in part by King Fahd University of Petroleum and Minerals through the KAUST004 grant, in part by King Saud University, Deanship of Scientific Research through the RG-1438-092 grant, and in part by KACST-TIC in SSL. M. Z. M. K gratefully acknowledges contributions from Prof. B. S. Ooi, Dr. T. K. Ng, Prof. P. Bhattacharya, and Dr. C-S. Lee.

References

1. M. A. Esmail, A. Ragheb, H. Fathallah, and M.-S. Alouini, in *IEEE International Conference on Communications Workshops (ICC)* (2016).
2. Y. Ren, Z. Wang, P. Liao, L. Li, G. Xie, H. Huang, Z. Zhao, Y. Yan, N. Ahmed, M. Lavery, and N. Ashrafi, in *OSA, Optical Fiber Communication Conference* (2015).
3. M. A. Esmail, H. Fathallah, and M. S. Alouini, IEEE Photon. J. **9**, 1 (2017).
4. G. Parca and A. L. J. Teixeira, Opt. Eng. **52**, 11 (2015).
5. A. S. Hamza, J. S. Deogun, and D. R. Alexander, in *IEEE Global Communications Conference (GLOBECOM)* (2014).
6. K. Wang, A. Nirmalathas, C. Lim, E. Skafidas, and K. Alameh, Opt. Lett. **39**, 19 (2014).
7. F. Carvalho and C. Cartaxo, IEEE Photon. Tech. Lett. **27**, 1193 (2015).
8. D. J. Shin, Y. C. Keh, J. W. Kwon, E. H. Lee, J. K. Lee, M. K. Park, J. W. Park, Y. L. Oh, S. W. Kim, I. K. Yun, and H. C. Shin, J. Lightwave Technol. **24**, 1 (2006).
9. E. Wong, J. Lightwave Technol. **30**, C4 (2012).
10. J. N. Kemal, K. Merghem, G. Aubin, and C. Calo, in *Optical Fiber Communications Conference and Exhibition (OFC)* (2017).
11. Q. T. Nguyen, P. Besnard, L. Bramerie, A. Shen, C. Kazmierski, P. Chanlou, G. H. Duan, and J. C. Simon, IEEE Photon. Tech. Lett. **22**, 11 (2010).
12. M. Chen, J. He, and L. Chen, J. Opt. Commun. Networking **6**, 1 (2014).
13. M. T. A. Khan, M. A. Shemis, A. M. Ragheb, M. A. Esmail, H. Fathallah, S. Alshebeili, and M. Z. M. Khan, IEEE Photon. J. **9**, 1 (2017).
14. M. Z. M. Khan, T. K. Ng, C. Lee, P. Bhattacharya, and B. S. Ooi, IEEE J. Quantum Electron. **50**, C2 (2014).
15. H. Kaushal, V. K. Jain, and S. Kar, *Free Space Optical Communication* (Springer, 2017).